Cancer Chemother Pharmacol (1995) 37: 173–178

ORIGINAL ARTICLE

Glenn J. Lesser · Stuart A. Grossman · Susan Eller
Eric K. Rowinsky

The distribution of systemically administered [3H]-paclitaxel in rats: a quantitative autoradiographic study

Received: 14 October 1994 / Accepted: 28 February 1995

Abstract Paclitaxel is an important agent in the treatment of many common malignancies. Although the symptomatic peripheral neuropathy caused by this drug is its principal nonhematologic toxicity, little is known about the distribution of paclitaxel within the peripheral or central nervous system following systemic administration. In order to study paclitaxel's distribution in neural and extraneural tissues, adult Sprague-Dawley rats were sacrificed 2 h after a tail vein injection of [3H]-paclitaxel (0.03 mg/kg, 250 μCi/rat). Samples of lung, heart, liver, spleen, kidney, skeletal muscle, brain, spinal cord, dorsal root ganglion, and peripheral nerve were then removed and snap-frozen. These tissues were sectioned at 10 μm in a cryostat and exposed to autoradiography film for 2 weeks. The distribution and concentrations of [3H]-paclitaxel in plasma, urine and cerebrospinal fluid were also determined using liquid scintillation spectrometry. [3H]-Paclitaxel concentrations (and organ/plasma concentration ratios) in plasma, urine and cerebrospinal fluid were 2.6 n*M* (1), 38 n*M* (15) and 0.7 n*M* (0.3), respectively. A relatively homogeneous distribution of [3H]-paclitaxel was observed in liver [412 n*M* (151)], spleen [351 n*M* (133)], heart [319 n*M* (117)], lung [268 n*M* (93)] and muscle [69 n*M* (26)]. Higher concentrations of [3H]-paclitaxel were noted in the portal triads [869 n*M* (361)], glomeruli [797 n*M* (304)], and renal medulla [961 n*M* (363)], which may reflect biliary excretion and glomerular filtration. A high concentration of [3H]-paclitaxel was also noted in the choroid plexus [432 n*M* (167)], but [3H]-paclitaxel was not detected in the brain parenchyma, spinal cord, dorsal root ganglion, peripheral nerve, or the testicles. The pathogenesis of paclitaxel-induced neurotoxicity remains obscure given its limited distribution in the nervous system. In addition, these results suggest that systemically administered paclitaxel is not likely to be effective for the treatment of malignancies in the testes or the nervous system.

Key words Paclitaxel · Peripheral neuropathy · Tissue distribution

Introduction

Peripheral neurotoxicity is the principal nonhematologic toxicity of paclitaxel [12, 20, 27], the prototypic taxane agent which has demonstrated significant antineoplastic activity in patients with advanced ovarian [13, 18, 25], breast [9, 16], lung [3, 6], and head and neck [7] cancers. This is likely to result from the formation of unusually stable and dysfunctional microtubules that occur following administration of this agent [23]. Most patients receiving repeated courses of paclitaxel at conventional doses (135–200 mg/m^2 over 24 h) will develop a symptomatic peripheral neuropathy [4, 12, 26, 27]. This is generally profound in patients receiving multiple courses of paclitaxel at doses above 250 mg/m^2 administered over 3 or 24 h [22, 24]. In addition, a peripheral neuropathy is the dose-limiting toxicity when paclitaxel is given as a single agent or with cisplatin at higher doses in combination with hematopoietic colony-stimulating factors [20, 22].

Paclitaxel produces primarily a sensory and motor polyneuropathy and only rarely do manifestations of autonomic or central nervous system dysfunction occur [19]. The available data suggest that paclitaxel produces a toxic effect on axons or ganglion cell bodies, or both, rather than a myelinopathy [21]. The time course of paclitaxel-induced neurotoxicity is variable and is related to dose level and the cumulative dose administered. While the relative incidence of neurotoxicity with a 3-h versus a 24-h paclitaxel infusion is not yet clear, the dose-limiting toxicity at the maximum tolerated dose is neurotoxicity with both schedules of administration [24].

G.J. Lesser · S.A. Grossman · S. Eller · E.K. Rowinsky
The Johns Hopkins Oncology Center, Baltimore, MD 21287, USA

S.A. Grossman (✉)
The Johns Hopkins Oncology Center, 600 North Wolfe Street, Baltimore, MD 21286, USA

Despite the clinical importance of paclitaxel-induced neurotoxicity and the prominent activity of paclitaxel in tumors that commonly metastasize to the central nervous system (e.g. breast and lung carcinomas), there is limited information regarding its penetration into the central or peripheral nervous system. Understanding paclitaxel's penetration across the blood-brain and blood-nerve barriers may facilitate the development of strategies to prevent neurotoxicity or to enhance drug delivery into the central nervous system in patients in whom that is appropriate.

This study was designed to quantify the tissue distribution of paclitaxel following intravenous administration in rats. [^{3}H]-Paclitaxel was administered and quantitative autoradiography from thin sections of various neural and non-neural tissues was performed. [^{3}H]-Paclitaxel concentrations, tissue-to-plasma concentration ratios, and the local distribution of the radiolabelled drug were determined in each tissue that was evaluated.

Materials and methods

Preparation of [^{3}H]-paclitaxel for injection

[^{3}H]-Paclitaxel in toluene (specific activity 23 Ci/mmol) was obtained from Moravek Biochemicals (Brea, Calif.) and stored at −70 °C. This preparation contained a mixture of [^{3}H]-paclitaxel species with tritium labels distributed throughout the taxane ring, aromatic rings, and the C-13 side chain. On average, each paclitaxel molecule contained ≤1 tritium label. The [^{3}H]-paclitaxel was prepared for intravenous administration by allowing the drug to warm to room temperature and then evaporating the toluene under a stream of nitrogen gas. The [^{3}H]-paclitaxel was resuspended in DMSO or 10% ethanol/10% Cremophor EL (polyoxyethylated castor oil, Sigma Chemical Company, St. Louis, Mo.) (v/v) in 0.9% saline and stored at −20 °C. Thin layer chromatography (silica gel plate; 1:1 acetonitrile/methanol solvent) of the resuspended tritiated compound demonstrated similar radiolabelled drug activity and migration in the DMSO, Cremophor, and toluene solvents.

Administration of intravenous [^{3}H]-paclitaxel

All animal care and experiments were performed in accordance with the guidelines set forth by the Animal Care and Use Committee of the Johns Hopkins Medical Institutions. Four male Sprague-Dawley rats (280–312 g) were anesthetized with inhaled Metafane (Pitman-Moore, Washington Crossing, N.J.) and given 10 μg (0.03 mg/kg) of [^{3}H]-paclitaxel by tail vein injection. The first rat received 125 μl [^{3}H]-paclitaxel (250 μCi) in DMSO followed by 375 μl of 0.9% saline over 1–2 min. This produced ataxia and sedation which resolved 1 h after the injection. This rat was sacrificed 2 h following injection with an intraperitoneal injection of pentobarbital. Ataxia and sedation of a similar degree and duration were seen in a control rat given the DMSO solvent alone. Thereafter, rats were treated with tail vein injections of 250 μCi of [^{3}H]-paclitaxel in 250 μl Cremophor vehicle followed by 250–300 μl 0.9% saline to flush the injection line. These animals did not exhibit ataxia or sedation and were sacrificed 2 h after drug administration with an intracardiac injection of pentobarbital. Immediately after death, the heart, lungs, liver, spleen, kidneys, testes, brain, cervical spinal cord, sciatic nerve, lumbar dorsal root ganglia (L4–L6), and a wedge of hindlimb skeletal muscle were removed and snap-frozen in hexane at −40 °C. All tissues were stored at −20 °C prior to sectioning.

Samples of blood, urine and cerebrospinal fluid were also collected at the time the animals were sacrificed. Whole blood samples were placed in glass tubes containing lithium heparin and centrifuged at 2500 rpm for 10 min. Plasma was removed and stored in polypropylene tubes at −20 °C. Urine and cerebrospinal fluid were centrifuged in polypropylene microcentrifuge tubes for 5 min and stored at −20 °C.

Preparation of tissues for quantitative autoradiography

Frozen organs and tissue samples were mounted on cryostat chucks with embedding matrix (OCT Compound; Miles, Elkhart Ind.) and cut into 10 μm sections in a cryostat (Hacker Instruments, Fairfield, N.J.) at −17 °C. Six pairs of consecutive sections were randomly selected from each organ or tissue sample. One section from each pair was mounted on a gelatin-coated slide and stained with hematoxylin and eosin for histologic review. The second section was thaw-mounted on a gelatin-coated glass slide warmed to 60 °C and was used for quantitative autoradiography. Slides for autoradiography were heat-fixed on a slide warmer for 15 min after preparation.

Tritium standards (Amersham Corp., Arlington Heights, Ill.) with eight levels of activity (6660 to 244, 200 dpm/mg tissue) and the slides containing the tissue sections for quantitative autoradiography were placed against tritium-sensitive film (Ultrofilm; Leica, Deerfield, Ill.) in an X-ray cassette and exposed for 2 weeks at room temperature. The films were developed for 5 min at room temperature (D-19 Developer; Kodak, Rochester, N.Y.), placed in a stop bath (Kodak) for 30 s, immersed in fixer (Kodak) for 5 min and exposed to flowing room temperature water for 10–15 min. They were then rinsed in Photo-Flo 200 (Kodak) and allowed to air dry.

Quantitative autoradiography analysis

The autoradiographs and tritium standards were digitized on an RAS-R1000 Receptor Autoradiography Analysis System (Loats Associates, Westminster, Md.). The optical densities of the tritium standards were corrected for background and used to generate a curve to convert optical density data into disintegrations per minute per milligram of tissue. A power function using least-squares regression of the optical densities of the tritium standards provided the highest coefficient of determination ($r^2 > 0.99$). Using the known specific activity of [^{3}H]-paclitaxel, disintegrations per minute per milligram of tissue were converted into femtomoles of paclitaxel per milligram of tissue or nanomolar concentrations.

Four autoradiographic images from different regions of each organ or tissue sample were digitized from each animal. The optical densities of these images were used to calculate organ or tissue mean and regional [^{3}H]-paclitaxel concentrations. The optical density of the entire specimen was averaged in organs or tissues with homogeneous drug distribution as evidenced by minimal variation in the optical density of the autoradiographic image. For tissues with significant regional differences in [^{3}H]-paclitaxel distribution, such as the kidney, the average optical density of each region of interest was calculated separately.

In these experiments, the optical density of the least-active tritium standard was equivalent to a [^{3}H]-paclitaxel concentration of approximately 100 n*M*. However, tissues with a [^{3}H]-paclitaxel concentration ≥30 n*M* were reproducibly visualized and measured by the digitizing software. Despite the use of a 0-n*M* standard (background), [^{3}H]-paclitaxel tissue concentrations between 30 n*M* and 100 n*M* fell on the tail of the standard curve and were therefore subject to greater measurement error.

Plasma, urine and cerebrospinal fluid analysis

Samples of plasma, urine and cerebrospinal fluid were allowed to warm to room temperature prior to analysis. ACS scintillation cocktail (15 ml) (Amersham, Arlington Heights, Ill.) was added to duplicate samples of each body fluid (100 μl plasma, 25–50 μl urine, or 25 μl CSF). Samples were counted in a Beckman LS8000 Liquid Scintillation Counter (Beckman Instruments, Columbia, Md.) for 1 min. Counts per minute were converted to disintegrations per minute using a

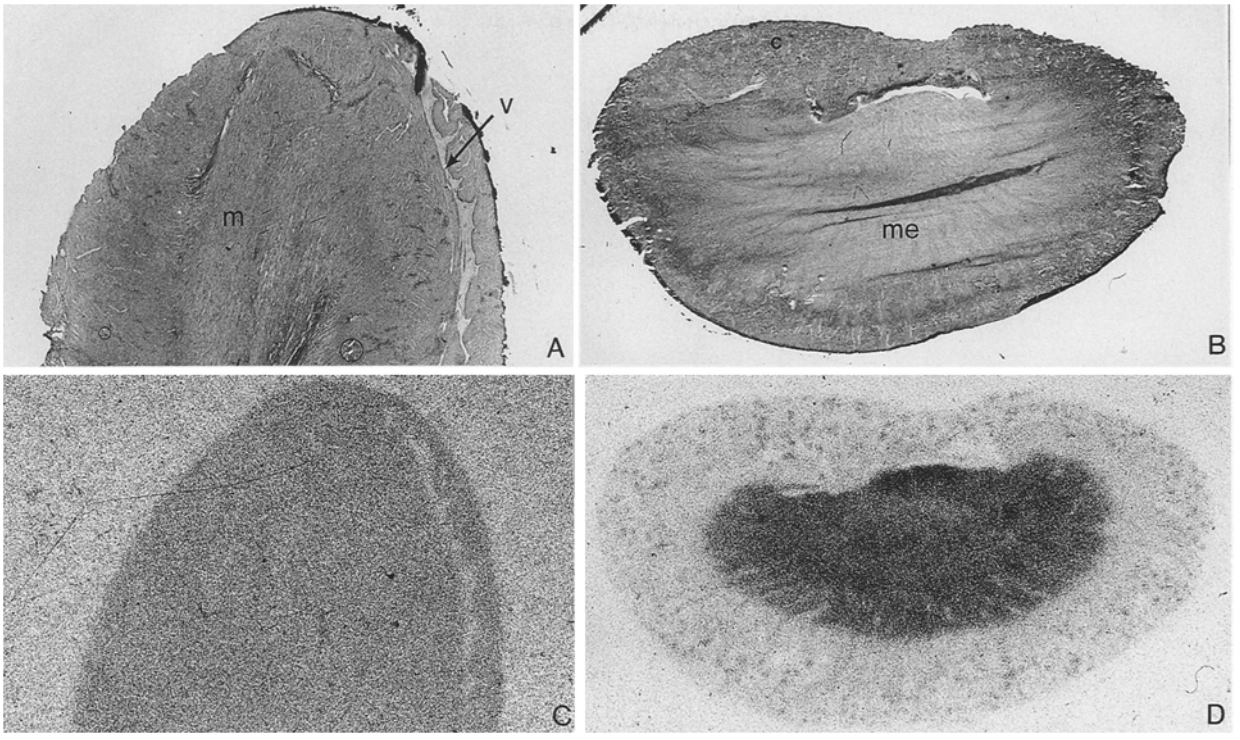

counting efficiency of 50% which was determined by counting ^{3}H standards. The concentration of [^{3}H]-paclitaxel in each fluid was calculated using the known specific activity of the administered [^{3}H]-paclitaxel.

Fig. 1 A–D H&E-stained sections (**A, B**) and the corresponding autoradiographs (**C, D**) of the heart (**A, C**) and kidney (**B, D**) of a rat, 2 h after a tail vein injection of [^{3}H]-paclitaxel (0.03 mg/kg, 250 μCi). The autoradiograph of the heart (**C**) demonstrates homogeneous [^{3}H]-paclitaxel distribution while in the kidney (**B, D**) the renal medulla (*me*) and glomeruli contain significantly higher [^{3}H]-paclitaxel concentrations than the renal cortex (*c*) (*v* ventricles, *m* myocardions)

Table 1 [^{3}H]-Paclitaxel Organ concentrations[a] and organ-to-plasma concentration ratios in the rat 2 hours after a tail vein injection (250 μCi, 0.03 mg/kg). The concentration values are the means (and SD) of the averages from each animal (*ND* none detected)

Tissue	n*M* (SD)	Organ/plasma (SD)
Plasma	2.6 (0.5)	1
Urine	38 (15)	15 (5)
Cerebrospinal fluid	0.7 (0.2)	0.3 (0.1)
Nervous system		
Cerebrum	ND	ND
Choroid plexus	432 (203)	167 (51)
Spinal cord	ND	ND
Dorsal root ganglion	ND	ND
Testes	ND	ND
Muscle	69 (25)	26 (5)
Lung	268 (95)	93 (34)
Heart	319 (184)	117 (54)
Spleen	351 (210)	133 (64)
Liver		
Average	412 (279)	151 (84)
Portal triad	869 (75)	361 (48)
Kidney		
Average	484 (274)	183 (82)
Renal cortex	251 (120)	94 (34)
Glomerulus	797 (214)	304 (40)
Renal medulla	961 (462)	363 (133)

[a] Four autoradiographic images from different regions of each organ or tissue sample were digitized from each animal and averaged.

Results

[^{3}H]-Paclitaxel tissue concentrations and tissue-to-plasma ratios for the tissues and body fluids examined are displayed in Table 1. The observed counts-per-minute of the individual urine, plasma and CSF samples (and the counting error for those samples as calculated by the scintillation counter) were 20,200–40,432 (± 1.7–1.8%), 2258–7772 (± 2.2–4.2%), and 337–547 (± 8.5–10.8%), respectively.

The highest concentrations of [^{3}H]-paclitaxel were noted in the liver, spleen, heart, lung, and kidney. Organ-to-plasma concentration ratios of 94 to 183 were found in these tissues 2 h after drug administration. In contrast, [^{3}H]-paclitaxel could not be detected in brain parenchyma, cervical spinal cord, lumbar dorsal root ganglia, sciatic nerve, or the testes of the experimental animals. Quantitative autoradiographic image analysis revealed a relatively homogeneous distribution of [^{3}H]-paclitaxel throughout the heart (Fig. 1a, c), most of the liver parenchyma, spleen, and skeletal muscle. The drug was also distributed homogeneously throughout lung parenchyma, but was absent in alveolar airspaces.

In contrast, several organs contained regions of higher [^{3}H]-paclitaxel concentrations. Within the kidney, two well-demarcated, homogeneous zones of increasing [^{3}H]-pacli-

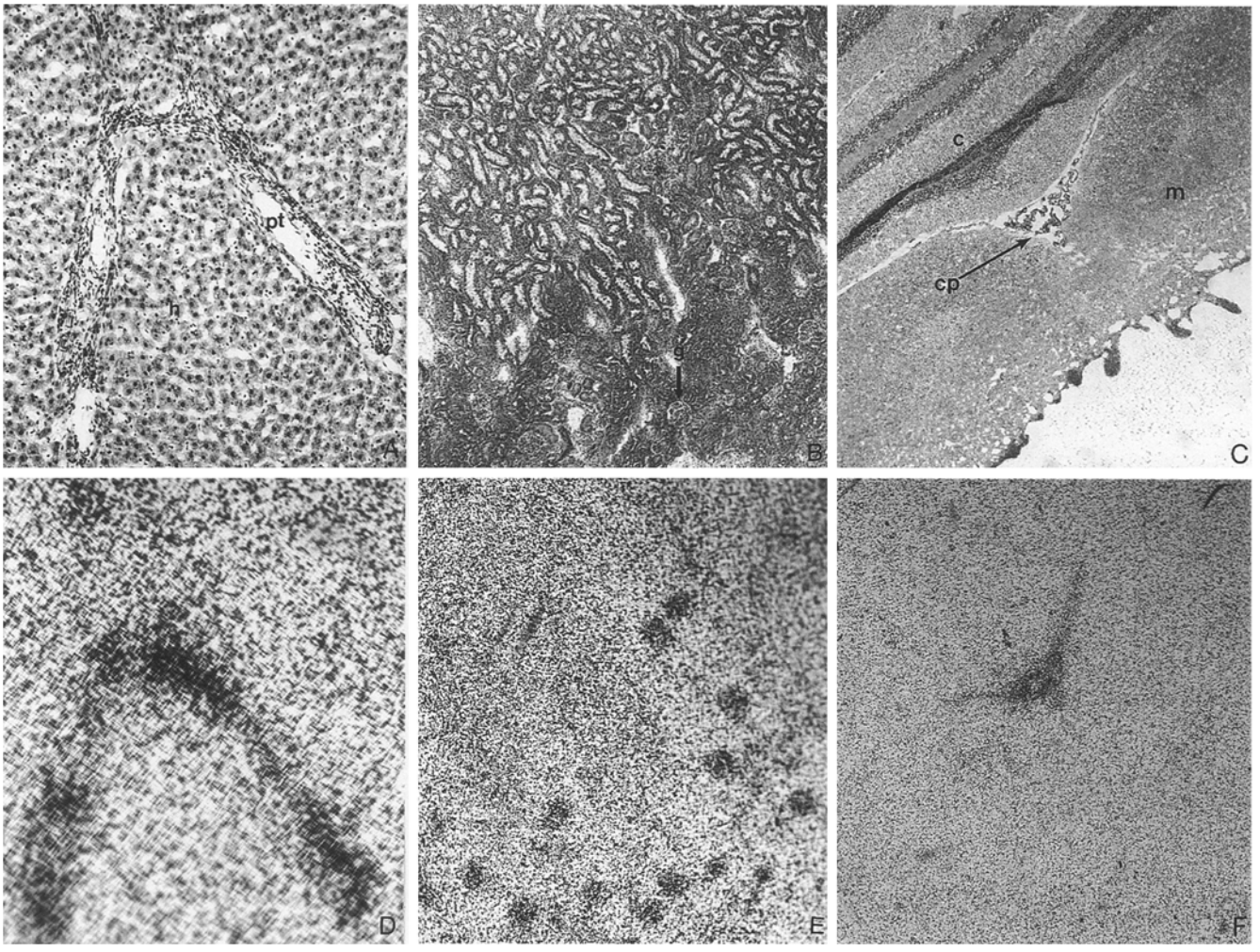

Fig. 2 A–F Regions of high [^{3}H]-paclitaxel concentration 2 h after a tail vein injection (0.03 mg/kg, 250 μCi) in the rat. H&E-stained sections (**A, B, C**) and the corresponding autoradiographs (**D, E, F**) of a portal triad (**A, D**), glomeruli (**B, E**) and the choroid plexus of the fourth ventricle (**C, F**) are shown (*h* hepatic parenchyma, *pt* portal triad, *g* glomerulus, *c* cerebellum, *cp* choroid plexus, *m* midbrain

taxel concentrations were identified (Fig. 1b,d). These corresponded to the renal cortex and medulla as assessed by light microscopy. In addition, numerous small foci of high [^{3}H]-paclitaxel concentration were distributed throughout the outer cortex of the kidney. These regions were identified as glomeruli by light microscopy (Fig. 2b,e). Within the liver, foci of higher [^{3}H]-paclitaxel concentrations corresponded to the portal triads (Fig. 2a,d). High [^{3}H]-paclitaxel concentrations were also noted in the choroid plexus of the fourth ventricle in the brain of these animals (Fig. 2c,f).

Discussion

These quantitative autoradiographic studies provide a unique view of the tissue distribution of systemically administered [^{3}H]-paclitaxel. They demonstrate that this agent is widely distributed with high concentrations and high tissue-to-plasma concentration ratios in a broad range of tissues 2 h after intravenous administration in rats. These results are consistent with those reported by Klecker et al. who performed tissue distribution studies in rats using organ-digest methods and a 6-h continuous infusion of 2 mg/kg of [^{3}H]-paclitaxel [11]. High tissue-to-plasma concentration ratios were noted in liver, kidney, spleen, lung and heart while negligible concentrations were found in brain and testes.

Both quantitative autoradiography and organ-digest studies are useful in quantifying the tissue distribution of radiolabelled drugs like paclitaxel. However, quantitative autoradiography allows visualization and quantification of drug distribution within tissues of interest. The study reported here reveals increased [^{3}H]-paclitaxel within portal triad, glomerulus, renal medulla, and choroid plexus.

The demonstration of high [^{3}H]-paclitaxel concentrations within the portal triads of the liver in this study is consistent with reports indicating that hepatic metabolism and biliary excretion is a principal mechanism of paclitaxel elimination [14]. Monsarrat et al. demonstrated that biliary excretion of parent compound and several hydroxylated metabolites accounts for 40% of total drug disposition 24 h

after intravenous administration in rats. In contrast, only 10% of the administered drug was recovered as the parent compound in rat urine over this same period, and urinary metabolites were not detected. Although high concentrations of [3H]-paclitaxel were found in the kidney and urine in this study, data from a single sampling point post-treatment cannot be used to reliably assess the significance of cumulative renal [3H]-paclitaxel disposition over time.

The accumulation of [3H]-paclitaxel in the choroid plexus and not within the brain parenchyma demonstrates that, despite its lipid solubility, paclitaxel entry into the central nervous system is impeded by the blood-brain barrier. This observation is supported by other studies evaluating the tissue distribution of paclitaxel in mice and rats [5, 11]. In humans, the only data on the penetration of this agent within normal brain come from a single report in which paclitaxel could not be identified in the cerebrospinal fluid of patients with leukemia following high-dose (390 mg/m^2) intravenous administration [17]. Additionally, central nervous system toxicity has only rarely been reported in patients who have received this agent [18, 19].

The inability to detect [3H]-paclitaxel within the peripheral nervous system in this study is of interest in view of the clinical neurotoxicity induced by this agent. There are several possible explanations for this apparent discrepancy. First, it is possible that the concentration of paclitaxel within the nervous system was lower than the lower limit of detection of this quantitative autoradiographic approach. Second, plasma [3H]-paclitaxel concentrations may not have been sufficiently high or sustained to promote the diffusion of drug across the blood-nerve barrier in these experimental animals. The blood-nerve barrier is similar to the blood-brain barrier. Uncharged, low molecular mass, lipid-soluble compounds diffuse through the lipid bilayer of the perineurium and the nonfenestrated endothelium of the endoneurial vasculature [15]. This diffusion is known to be concentration dependent [15] and therefore limited by the absolute and cumulative plasma paclitaxel concentrations generated in the experimental animals. An identical relationship between cumulative drug exposure and the resulting drug concentration in spinal ganglia and peripheral nerves has been reported for cisplatin, another neurotoxic chemotherapeutic agent [8].

Compounds can also reach the nerves, bypassing the blood-nerve barrier, via uptake at the motor endplate followed by retrograde axonal transport. This has been noted with doxorubicin. This agent has been detected in hypoglossal and trigeminal neurons 6 h after intramuscular or intradermal injections into the tongue, masseter and cheek [2]. It is not known if paclitaxel can bypass the blood-nerve barrier in this manner or if paclitaxel concentrations in synaptic clefts are high enough to make this a reasonable possibility. However, the autoradiographic studies do demonstrate measurable concentrations of paclitaxel in skeletal muscle.

Finally, the inability to detect [3H]-paclitaxel within the peripheral nervous system may indicate that the paclitaxel-induced neuropathy is caused by a metabolite that does not contain a tritium label. This is unlikely since all paclitaxel metabolites identified using analytical HPLC, spectrometry, and NMR spectroscopy are mono- or dihydroxylated derivatives with intact side chains at both the C2 and C13 positions [14]. In addition, the [3H]-paclitaxel preparation used in these experiments contained a mixture of [3H]-paclitaxel species with tritium labels distributed throughout the taxane ring, aromatic rings, and the C-13 side chain. However, since not all [3H]-paclitaxel molecules were labelled in all available positions, tritium-labelled metabolites may have been generated in the experimental animals in concentrations below the limit of detection of quantitative autoradiography.

[3H]-Paclitaxel distribution to rat testis was also demonstrated to be lower than the limit of our autoradiographic technique. This is consistent with reports from other investigators in which [3H]-paclitaxel was detected in negligible amounts in the testis of rats and CD2F1 mice after treatment [5, 11]. Human evidence for a barrier to testicular penetration of paclitaxel is limited to a single report of three patients with acute myelogenous leukemia who had no evidence of paclitaxel-induced mitotic arrest or chromosomal changes within the testes at their post-mortem examination performed 1 to 27 days after treatment with paclitaxel [10]. However, markedly reduced numbers of germ cells (i.e. fewer cells in which to see paclitaxel-induced mitotic arrest or chromosomal changes) were present in the testes from these patients, presumably secondary to prior chemotherapy administration.

In summary, these autoradiographic studies demonstrate extensive tissue binding of [3H]-paclitaxel within the liver, spleen, kidney, heart, lung, and skeletal muscle of rats after bolus intravenous infusion. In most organs the [3H]-paclitaxel was distributed homogeneously; however, high concentrations were found in the portal triad, glomerulus and renal medulla which may be accounted for by substantial biliary excretion and glomerular filtration. Drug concentration was also high in the choroid plexus. As paclitaxel was not detected in the central or peripheral nervous system, the etiology of the drug-induced neurotoxicity remains unclear. A murine model of paclitaxel-induced peripheral neurotoxicity utilizing repeated intraperitoneal administration of paclitaxel has been described [1]. Quantitative autoradiographic analysis of the peripheral nervous system in these animals with established neuropathies might clarify the mechanism of this neurotoxicity.

The low concentrations of this agent within the nervous system and the testes suggests that paclitaxel therapy may be suboptimal in clinical situations requiring therapeutic drug levels in these sanctuary sites. In addition, a more thorough understanding of paclitaxel's distribution within the central nervous system in the presence of an intact and disrupted blood-brain barrier is required if the activity of this drug against primary and metastatic brain tumors is to be pursued.

References

1. Apfel SC, Lipton RB, Arezzo JC, Kessler JA (1991) Nerve growth factor prevents toxic neuropathy in mice. Ann Neurol 29:87–90
2. Bigotte L, Olsson Y (1984) Cytotoxic effects of adriamycin on the central nervous system of the mouse – cytofluorescence and electron-microscopic observations after various modes of administration. Acta Neurol Scand 70 [Suppl 100]:55–67
3. Chang AY, Kim K, Glick J, Anderson T, Karp D, Johnson D (1993) Phase II study of taxol, merbarone, and piroxantrone in stage IV non-small-cell lung cancer: the Eastern Cooperative Oncology Group results. J Natl Cancer Inst 85:388–394
4. Donehower RC, Rowinsky EK, Grochow LB, Longnecker SM, Ettinger DS (1987) Phase I trial of taxol in patients with advanced cancer. Cancer Treat Rep 71:1171–1177
5. Eiseman JL, Eddington N, Leslie J, MacAuley C, Sentz D, Kujawa J, Zuhowski M, Haidir S, Young D, Egorin MJ (1993) Pharmacokinetics and development of a physiologic model of taxol in CD2F1 mice (abstract). Proc Am Assoc Cancer Res 34:396
6. Ettinger DS (1993) Taxol in the treatment of lung cancer. Monogr Natl Cancer Inst 15:177–179
7. Forastiere AA, Neuberg D, Taylor SG, Deconti R, Adam G (1993) Phase II evaluation of taxol in advanced head and neck cancer: an Eastern Cooperative Oncology Group trial. Monogr Natl Cancer Inst 15:181–184
8. Gregg RW, Molepo JM, Monpetit JA, Mikael NZ, Redmond D, Gadia M, Stewart DJ (1992) Cisplatin neurotoxicity: the relationship between dosage, time, and platinum concentration in neurologic tissues, and morphologic evidence of toxicity. J Clin Oncol 10:795–803
9. Holmes FA, Walters RS, Theriault RL, Forman AD, Newton LK, Raber MN, Buzdar AU, Frye DK, Hortobagyi GN (1991) Phase II trial of taxol, an active drug in the treatment of metastatic breast cancer. J Natl Cancer Inst 83:1797–1805
10. Hruban RH, Yardley JH, Donehower RC, Boitnott JK (1989) Taxol toxicity: Epithelial necrosis in the gastrointestinal tract associated with polymerized microtubule accumulation and mitotic arrest. Cancer 63:1944–1950
11. Klecker RW, Jamis-Dow CA, Egorin MJ, Erkmen K, Parker RJ, Stevens R, Collins JM (1994) Effect of cimetidine, probenecid and ketoconazole on the distribution, biliary secretion and metabolism of 3H-taxol in the Sprague-Dawley rat. Drug Metab Dispos 22:254–258
12. Lipton RB, Apfel SC, Dutcher JP, Rosenberg R, Kaplan J, Berger A, Einzig AI, Wiernik P, Schaumburg HH (1989) Taxol produces a predominantly sensory neuropathy. Neurology 39:368–373
13. McGuire WP, Rowinsky EK, Rosenshein NB, Grumbine FC, Ettinger DS, Armstrong DK, Donehower RC (1989) Taxol: a unique antineoplastic agent with significant activity in advanced ovarian epithelial neoplasms. Ann Intern Med 111:273–279
14. Monsarrat B, Alvinerie P, Wright M, Dubois J, Guéritte-Voegelein F, Guénard D, Donehower RC, Rowinsky EK (1993) Hepatic metabolism and biliary excretion of taxol in rats and humans. Monogr Natl Cancer Inst 15:39–46
15. Rechthand E, Rapoport SI (1987) Regulation of the microenvironment of peripheral nerve: role of the blood-nerve barrier. Prog Neurobiol 28:303–343
16. Reichman BS, Seidman AD, Crown JPA, Heelan R, Hakes TB, Lebwohl DE, Gilewski TA, Surbone A, Currie V, Hudis CA, Yao TJ, Klecker R, Jamis-Dow C, Collins J, Quinlivan S, Berkery R, Toomasi F, Canetto R, Fisherman J, Arbuck S, Norton L (1993) Paclitaxel and recombinant human granulocyte colony-stimulating factor as initial chemotherapy for metastatic breast cancer. J Clin Oncol 11:1943–1951
17. Rowinsky EK, Burke PJ, Karp JE, Tucker RW, Ettinger DS, Donehower RC (1989) Phase I and pharmacodynamic study of taxol in refractory acute leukemias. Cancer Res 49:4640–4647
18. Rowinsky EK, Cazenave LA, Donehower RC (1990) Taxol: a novel investigational antimicrotubule agent. J Natl Cancer Inst 82:1247–1259
19. Rowinsky EK, Chaudhry V, Cornblath DR, Donehower RC (1993) Neurotoxicity of taxol. Monogr Natl Cancer Inst 15:107–115
20. Rowinsky EK, Chaudhry V, Forastiere AA, Sartorius SE, Ettinger DS, Grochow LB, Lubejko BG, Cornblath DR, Donehower RC (1993) Phase I and pharmacologic study of paclitaxel and cisplatin with granulocyte colony-stimulating factor: neuromuscular toxicity is dose-limiting. J Clin Oncol 11:2010–2020
21. Sahenk Z, Barohn R, New P, Mendell JR (1994) Taxol neuropathy: electrodiagnostic and sural nerve biopsy findings. Arch Neurol 51:726–729
22. Sarosy G, Kohn E, Stone DA, Rothenberg M, Jacob J, Adamo DO, Ognibene FP, Cunnion RE, Reed E (1992) Phase I study of taxol and granulocyte colony-stimulating factor in patients with refractory ovarian cancer. J Clin Oncol 10:1165–1170
23. Schiff PB, Horwitz SB (1980) Taxol stabilizes microtubules in mouse fibroblast cells. Proc Natl Acad Sci U S A 77:1561–1565
24. Schiller JH, Storer B, Tutsch K, Arzoomanian R, Alberti D, Feierabend C, Spriggs D (1994) Phase I trial of 3-hour infusion of paclitaxel with or without granulocyte colony-stimulating factor. J Clin Oncol 12:241–248
25. Trimble EL, Adams JD, Vena D, Hawkins MJ, Friedman MA, Fisherman JS, Christian MC, Canetta R, Onetto N, Hayn R, Arbuck SG (1993) Paclitaxel for platinum-refractory ovarian cancer: results from the first 1,000 patients registered to National Cancer Institute referral center 9103. J Clin Oncol 11:2405–2410
26. Wiernik PH, Schwartz EL, Einzig A, Strauman JJ, Lipton RB, Dutcher JP (1987) Phase I trial of taxol given as a 24-hour infusion every 21 days: responses observed in metastatic melanoma. J Clin Oncol 5:1232–1239
27. Wiernik PH, Schwartz EL, Strauman JJ, Dutcher JP, Lipton RB, Paietta E (1987) Phase I clinical and pharmacokinetic study of taxol. Cancer Res 47:2486–2493